

Fission barriers of light nuclei

K. Grotowski and R. Pjaneta

*Institute of Physics, Jagellonian University, Reymonta 4, Cracow, Poland
and Institute of Nuclear Physics, Cracow, Poland*

M. Blann and T. Komoto

Lawrence Livermore National Laboratory, Livermore, California 94550

(Received 27 December 1988)

Experimental fission excitation functions for compound nuclei ^{52}Fe , ^{49}Cr , ^{46}V , and ^{44}Ti formed in heavy-ion reactions are analyzed in the Hauser-Feshbach/Bohr-Wheeler formalism using fission barriers based on the rotating liquid drop model of Cohen *et al.* and on the rotating finite range model of Sierk. We conclude that the rotating finite range approach gives better reproduction of experimental fission yields, consistent with results found for heavier systems.

I. INTRODUCTION

In the present work, we analyze fissionlike yields from nearly symmetric decay of light composite systems $^{52}\text{Fe}^*$, $^{49}\text{Cr}^*$, $^{46}\text{V}^*$, and ^{44}Ti (Refs. 1 and 2) in order to test several models of fission barriers of light nuclei at moderately high angular momenta. For a long time, the only set of fission barrier calculations for nuclei under rotation resulted from the rotating liquid drop model (RLDM) of Cohen, Plasil, and Swiatecki.³ Statistical model analyses of fission excitation functions for systems of mass 100–200 suggested that the RLDM barriers were somewhat higher than experimentally deduced results.^{4,5} Similar results were obtained by other authors for medium weight and heavy systems.^{6–8} A hint that such a conclusion should not be unexpected came from the early finite range barrier calculations of Krappe, Nix, and Sierk⁹ performed for nonrotating systems. This model differed from the sharp surface liquid drop model, in that an attractive force of finite range was permitted between nascent fragments at the fission saddle point. It was demonstrated that this effect could reproduce the experimentally deduced angular-momentum-dependent barrier decrements from RLDM by modeling the static finite range effect to rotating systems.⁵ Explicit finite range rotating liquid drop model (RFRM) calculations were done by Mustafa, Baisden, and Chandra,¹⁰ and by Sierk.¹¹ These models were shown to give good agreement with experimentally deduced barriers for systems formed in heavy ion bombardments with $A > 100$.^{12–18}

We wish to see if the conclusions stated above are valid in the much lower mass systems ($A \leq 52$) for which results were presented in Refs. 1 and 2. In that mass range experimental determination of fissionlike yields is much more difficult than for heavier nuclei for two principal reasons: the fissionlike cross sections are much smaller, and the charge separation between target and projectile is much lower, rendering division between deep inelastic and fissionlike products more difficult and ambiguous. In order to get reasonable fission yields in this mass region, one must use higher bombarding energies than those which are satisfactory for heavier, more fissile systems,

which introduces additional complications in interpretation due to secondary evaporation from fission fragments, and due to incomplete fusion contributions to the reaction cross sections. Several questions may be raised about analyzing these light mass fissionlike data via statistical decay models, as is done in this work. The first is one of the meaning of theoretical barriers if the systems are not stable against symmetry in the fission channel (i.e., below the Businaro-Galone point).¹⁹ The second question is whether the data do in fact represent systems for which the entrance channel trajectory results in a compound nuclear system which is inside the fission saddle point, or whether a “fast fission” trajectory, which is always outside the saddle point, is the mechanism primarily responsible for the experimentally observed yields.

As far as the first point is concerned, the fissioning nuclear systems in question are believed to be quite deformed structures connected with a relatively narrow neck.²⁰ When calculating transmission over a barrier for symmetric fission, we assume that due to such neck the mass asymmetry degree at freedom is frozen on the short path between the saddle and scission point, and consequently that the conditional saddle points may be treated as unconditional.

On the second point, as stated in Refs. 1 and 2, the observed fissionlike products are suggestive of a compound nucleus (CN) process. Also, trajectory calculations performed for three systems considered in this work support a fusion-fission mechanism.²⁰ We have selected experimental data on symmetric fission as most of the finite range liquid drop model predictions are made for the case of symmetric splitting.^{10,11}

We will give a very brief summary of the experimental data in Sec. II, since a complete description of the experimental program has been published.^{1,2} In Sec. III we review the statistical Hauser-Feshbach/Bohr-Wheeler calculations which will be used to predict the fission cross sections expected from the experiments and based on RLDM and RFRM barriers. Because incomplete fusion channels may also contribute to the fission yields, the statistical calculations must, in principle, sum over both complete and incomplete fusion channels. This problem

is discussed in Sec. III C. We will then present and discuss comparisons between calculated and experimental yields in Sec. IV, with a summary of our conclusions in Sec. V.

II. EXPERIMENTAL DATA AND THEIR INTERPRETATION

Fissionlike yields analyzed in this work were observed in reactions of ^{12}C , ^9Be , and ^6Li on ^{40}Ca , and of ^{32}S on ^{12}C targets.^{1,2} Measured cross sections and some parameters which characterize the corresponding reaction systems are shown in Table I. For all reactions in question, the presence of products with about one-half the mass of the compound nucleus ($A \sim 20$) does not prove the existence of a fission process. One can expect significant contributions from fusion evaporation residues or from reactions on light target contaminations at $A \sim 20$. In order to avoid most of these ambiguities, symmetric splitting of nuclei from Table I was verified by coincidence experiments. For $^{12}\text{C} + ^{40}\text{Ca} \rightarrow ^{52}\text{Fe}^*$ an excitation function has been measured in the range 57–147 MeV (c.m.); other reactions were investigated at different incident energies, 76–133 MeV (c.m.). As shown in Table I, fission cross sections are given for these three Z values, which, depending on the compound nucleus and incident energy, correspond to nearly symmetric splitting.

The data suggest that at least in the range of c.m. angles $45\text{--}115^\circ$, for $^{12}\text{C} + ^{40}\text{Ca}$, and $30^\circ\text{--}170^\circ$, for $^{32}\text{S} + ^{12}\text{C}$, the angular distribution is $\sim 1/\sin\Theta_{\text{c.m.}}$, which is expected from the symmetric decay of a system with a lifetime equal to or greater than a rotation period. Also, the excitation function measured for $^{12}\text{C} + ^{40}\text{Ca}$ supports a fusion/fissionlike process. The cross sections are larger for more symmetric configurations in the entrance channel. The measured total c.m. kinetic energies of fission products, together with the RLDM calculations, locate the window for symmetric decay at relatively high angu-

lar momenta ($30\hbar < L < 40\hbar$) where compound nuclei in question should be strongly deformed and slightly triaxial.

III. STATISTICAL CODES

The data described in Sec. II have been analyzed using the statistical code ALERT I of the Hauser-Feshbach-type, which includes the Bohr-Wheeler model for estimating the angular-momentum-dependent fission excitation functions. A detailed description of the equations governing these codes has been published elsewhere.^{4,21,22} We therefore present only a discussion of those details which are of particular relevance to the calculations performed for this work.

A. Fission barriers and transmission coefficients

Figure 1 compares angular-momentum-dependent fission barriers of the compound nucleus ^{52}Fe calculated using the RLDM (Cohen *et al.*³) and the RFRM (Sierk¹¹). It may be seen that the two models predict significantly different results. In the statistical calculations performed the barriers are recomputed for every nuclide in the decay chain, since multichance fission competition is considered.

The RLDM computes barriers for fission shapes with sharp surfaces. The RFRM refines the RLDM barriers by recomputation for systems with diffuse surfaces and an attractive force with a finite range between the adjacent surfaces of nascent fragments at the saddle point. The low mass nuclei, such as those considered in the present work, are expected to undergo fission only for relative high angular momenta (see Fig. 1) such that the fission barriers are not too much higher than the particle binding energies; otherwise, the phase space for particle emission completely dominates the decay process.

TABLE I. Summary of heavy ion reactions considered in this work. In addition to reacting nuclei, lab, and c.m. energy, the range of fragment charges included in experimental measurements are indicated for each composite system, as well as the composite nucleus excitation energy (E) given by $E_{\text{c.m.}} + Q$ and the temperature T deduced as $(E/a)^{1/2}$, where $a = A/8$ for $L = 0$.

Reaction	E_{lab} (MeV)	$E_{\text{c.m.}}$ (MeV)	Z fragments		Composite system	E (MeV)	T (MeV)
			included in σ_{fission}	σ_{fission} (mb)			
$^{12}\text{C} + ^{40}\text{Ca}^a$	186	143.1	9,10,11	21.6 ± 3.4	$^{52}_{26}\text{Fe}$	156.6	4.9
	161.9	124.5	9,10,11	23.3 ± 5.4		138.0	4.6
	131.9	101.5	9,10,11	12.9 ± 3.4		115.0	4.2
	121.3	93.4	10,11,12	17.2 ± 6.8		106.9	4.0
	74.3	57.1	10,11,12	2.2 ± 0.5		70.6	3.3
$^9\text{Be} + ^{40}\text{Ca}^a$	141	115.1	8,9,10	6.1 ± 1.7	$^{49}_{24}\text{Ca}$	136.9	4.7
$^6\text{Li} + ^{40}\text{Ca}^a$	153	109.3	8,9,10	5.6 ± 1.4	$^{46}_{23}\text{V}$	125.6	4.7
$^{32}\text{S} + ^{12}\text{C}^b$	280	76.4	9,10,11	6.1 ± 1.3	$^{44}_{22}\text{Ti}$	87.9	4.0

^aData taken from Ref. 1.

^bData taken from Ref. 2.

B. Level densities

In the statistical codes used in this work, angular-momentum-dependent level densities are calculated separately for each nuclide treated in the decay process, and for the fission channel. These level densities may be affected by nuclear deformation, and by so-called collective enhancement effects.²³ In our code, an option exists to compute these level densities using either a form appropriate to spherical nuclei, or a form for deformed nuclei with collective enhancement. Most important for level densities are the Fermi-gas level-density parameters for the ground state (a_v), and saddle-point nuclei (a_f). We have used saddle-point single-particle level densities based on the work of Bishop *et al.*²⁴ ($a_f/a_v=1.03$), although recent work of Leigh *et al.*¹³ in the $170 \leq A \leq 200$ region supports a somewhat lower value (~ 0.98). We have tested the sensitivity of results to the level-density parameter $a_v=A/8$ for particle emission with $a_f/a_v=0.98$ and 1.02 .

C. Input data

The statistical calculations require as input the angular momentum range and energies of excited nuclear species. The daughter excitation populations for the multichance fission competition following the xn , xp , and/or $x\alpha$ emission are generated internally, based on the initial excitation and range of angular momenta.

For the nuclear reactions considered, we expect that the entrance channels will have some range of partial waves undergoing compound nucleus formation. The corresponding angular momenta will be calculated from fusion cross sections using the sharp cutoff assumption. It is recognized that diffuse cutoffs are more realistic. However, there is no clear correct way in which to estimate these cutoffs, and the accuracy required for the purposes of this work does not require great attention to this point. We feel that the sharp cutoff approximation is adequate.

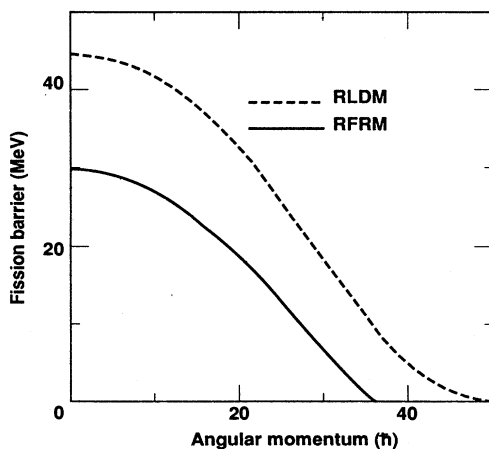


FIG. 1. Comparison of fission barrier vs angular momentum for ^{52}Fe calculated with the rotating liquid drop model (dashed line) and the finite range model (solid line).

In our case, fusion data exist only for the $^6\text{Li}+^{40}\text{Ca}$ reaction, for complete fusion, as well as for two main incomplete fusion channels.^{25,26} We have used the Bass model²⁷ to get fusion cross sections for $^{12}\text{C}+^{40}\text{Ca}$, $^9\text{Be}+^{40}\text{Ca}$, and $^{32}\text{S}+^{12}\text{C}$ reactions. In order to check the validity of Bass model predictions in our region of nuclei and energies we compared them (with success) with fusion evaporation residue cross sections measured for the $^{16}\text{O}+^{40}\text{Ca}$ reaction over a broad range of energies.²⁸

It is known that incomplete fusion increasingly competes with complete fusion at incident energies above 10 MeV/u. Unfortunately most of the published fusion data ($A_{\text{CN}} < 100$) give cross sections for the formation of the evaporation residues which is the sum of the cross section for complete and incomplete fusion. We shall call such cross sections the fusion cross sections. Recently, Morgenstern *et al.*²⁹ measured velocity spectra of evaporation residues for colliding systems having similar masses to those investigated in this work. For higher incident energies, velocity spectra deviate characteristically from the mean velocity of complete fusion. The authors determined the onset of incomplete fusion as a function of incident energy and mass asymmetry in the entrance channel. In Table II we show cross sections for fusion (σ_F) for the reactions in question, and cross sections for complete fusion (σ_{CF}) calculated mostly from the systematics of Morgenstern *et al.* The upper limit values of complete fusion angular momenta L_{CF} are presented in the last column. It should be pointed out that the Bass model was adjusted in order to reproduce the fusion data, and therefore it also needs the Morgenstern-type correction to provide the complete fusion cross section σ_{CF} .

As stated in Sec. I, the incomplete fusion channels may also participate in the fission yields. At 186 MeV (15.5 MeV/nucleon), more than 50% of the fusion cross section from the $^{12}\text{C}+^{40}\text{Ca}$ reaction belongs to incomplete fusion. One can expect that aside from complete fusion, the incomplete fusion reactions ($^{12}\text{C},\alpha$) and ($^{12}\text{C},^8\text{Be}$) will represent the dominant reaction channels. Adopting a simple reaction picture proposed by Siwek-Wilczynska *et al.*,³⁰ we assume that every virtual fragment of the projectile carries a part of the total angular momentum that

TABLE II. The fusion cross sections σ_F as predicted by the Bass model, and the corresponding complete fusion cross sections σ_{CF} , calculated according to Morgenstern *et al.* (Ref. 21). The L_{CF} values are given in the sharp cutoff approximation.

Reaction	E_{lab} (MeV)	σ_F (mb)	σ_{CF} (mb)	L_{CF} (\hbar)
$^{12}\text{C}+^{40}\text{Ca}$	186	1058	481	30.0
	161.9	1067	581	30.9
	131.9	1082	717	31.0
	121.3	1092	771	30.7
	74.3	1144	993	27.2
$^9\text{Be}+^{40}\text{Ca}$	141	1003	364	20.7
$^6\text{Li}+^{40}\text{Ca}$	153		67 ^a	7.4
$^{32}\text{S}+^{12}\text{C}$	280	1030	818	27.8

^aMeasured value from Ref. 17. The Bass model (Ref. 27) corrected according to Morgenstern *et al.* (Ref. 29) gives $\sigma_{\text{CF}}=62$ mb.

is proportional to its mass number. Consequently, for capture of ^8Be the lower angular momentum limit is $L'_{LL} = \frac{2}{3} \times 30\hbar = 20\hbar$, which value is nearly identical to the complete fusion upper limit L'_{CF} in the $^8\text{Be} + ^{40}\text{Ca}$ channel, as calculated from the Bass formula with the Morgenstern *et al.* correction included. This means that the $(^{12}\text{C}, \alpha)$ reaction channel is almost closed. It should be noticed that such conjecture is in agreement with both measurements and predictions of the more realistic sum-rule model of Wilczynski *et al.*,³¹ where only a small contribution was found at larger energies from incomplete fusion channels corresponding to the largest mass transfer. The $\alpha + ^{40}\text{Ca}$ fusion cross section was measured only up to 28 MeV (lab) (Ref. 32) and the Bass model predictions agree well with experimental data. For beam velocity α particles (62 MeV lab) the Bass model predicts a fusion cross section of 800 mb and the sharp cutoff approximation gives $14\hbar$ for the upper angular momentum. As will be seen from the statistical model calculations, we expect negligible fission yields from such low L partial waves. Consequently, we assume that there are no incomplete fusion contributions to the fission yields from the 186 MeV $^{12}\text{C} + ^{40}\text{Ca}$ system. It may be shown that the same is also valid for other reactions considered in this work.

IV. RESULTS

Comparison of statistical model predictions with experimental fission cross sections is presented for the $^{12}\text{C} + ^{40}\text{Ca}$ reaction in Figs. 2 and 3 and for the reactions $^9\text{Be}/^6\text{Li} + ^{40}\text{Ca}$, and $^{32}\text{S} + ^{12}\text{C}$ in Figs. 4 and 5. The rotating finite range model RFRM was the source of fission barriers used in calculations of Figs. 2 and 4 while the zero-range RLDM was utilized in Figs. 3 and 5. In each case, the sharp cutoff value of angular momentum L_{max} was optimized in order to fit the experimental data. The

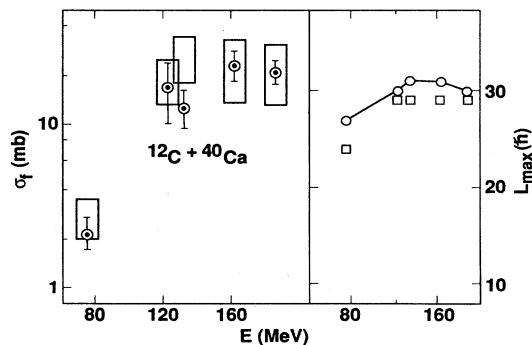


FIG. 2. Calculated and experimental fission cross sections vs ^{12}C projectile energy for a ^{40}Ca target. The ordinate on the left-hand portion of the figure shows experimental fission cross sections as circles with error bars. The rectangles give cross sections calculated using RFRM fission barriers with the ratio $a_f/a_v = 1.02$ (top of rectangle) and 0.98 (bottom of rectangle). The right-hand portion of the figure shows the L_{max} actually used in the calculations as open squares, and those predicted by Bass-Morgenstern as open circles connected by a solid line.

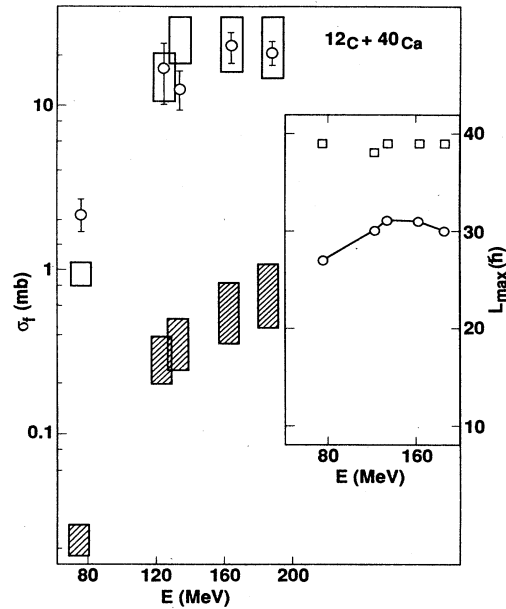


FIG. 3. As in Fig. 2, using fission barriers from the RLDM. The hatched rectangles result from using the L_{max} of Bass-Morgenstern (see the inset). The open rectangles result from using the adjusted L_{max} shown by the open squares of the inset.

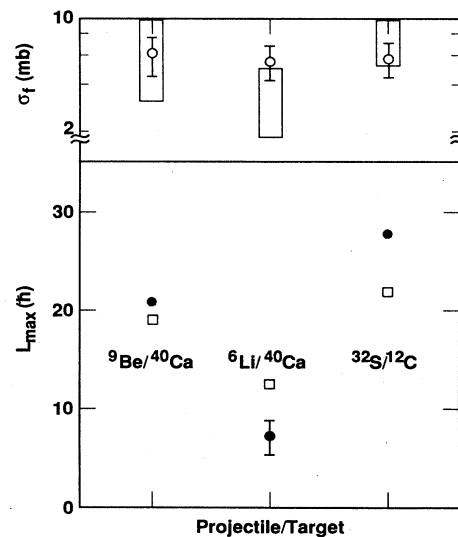


FIG. 4. Calculated vs experimental cross sections (upper figure) for several projectile/target combinations (abscissa). The rectangles are the range of results using RFRM barriers as in Fig. 2 with $a_f/a_v = 1.02$ and 0.98 . The lower portion of the figure shows the value of the angular momenta L_{max} used in the calculations (open square) and for $^9\text{Be} + ^{40}\text{Ca}$ and $^{32}\text{S} + ^{12}\text{C}$, the Bass-Morgenstern prediction. For $^6\text{Li} + ^{40}\text{Ca}$ the solid point with error bars represents the result deduced from $^6\text{Li} + \text{Ti}$ experimental measurement.

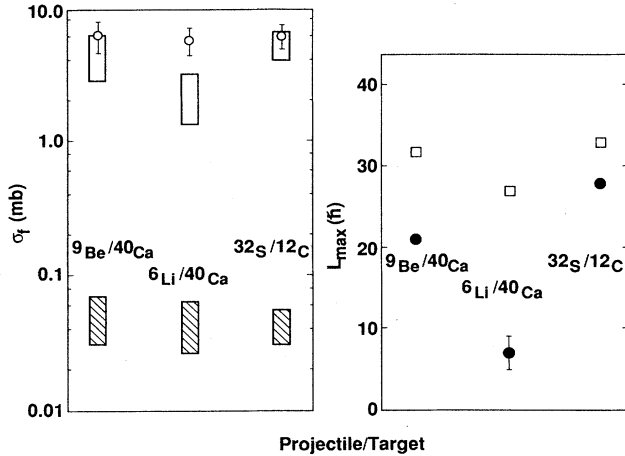


FIG. 5. As in Fig. 4, using the RLDM fission barriers. The open rectangles in the left-hand side of the figure represent the calculated results using L_{\max} given by the open squares on the right-hand side of the figure. The hatched rectangles are fission yields calculated using RLDM barriers with L_{\max} given by the solid points in the right-hand side of the figure. The extremes (top and bottom) of the rectangles correspond to $a_f/a_v = 1.02$ and 0.98, respectively.

(b) part of Figs. 2, 3, 4, and 5 presents the parameter fit values of L_{\max} compared to those suggested by the experimental fusion cross section or by the Bass model and the Morgenstern *et al.* systematics (see Sec. III C). Statistical model calculations were performed with the collective enhancement form of level densities and for the a_f/a_v ratio equal to 1.02 or 0.98 (the upper and the lower side of each rectangle in Figs. 2–5, respectively).

In the case of the $^{12}\text{C} + ^{40}\text{Ca}$ reaction, all fission cross sections could be satisfactorily reproduced using the RFRM fission barriers calculated for L_{\max} only slightly smaller (1 to 3 units of \hbar) than predicted by the Bass model and the Morgenstern *et al.* systematics [see Figs. 2(a) and 2(b)]. The largest difference ($3\hbar$) occurs at the lowest incident energy 74.3 MeV. The same L_{\max} values used in RLDM give fission cross sections more than an order of magnitude lower than experimental results [shaded rectangles in Fig. 3(a)]. In order to raise the statistical model predictions using RLDM barriers to the experimental values, we had to use L_{\max} values larger by more than $10\hbar$ from those used in the RFRM [see Fig. 3(b) and open rectangles in Fig. 3(a)].

The procedure used for $^{12}\text{C} + ^{40}\text{Ca}$ was also adopted for the remaining three reactions and is illustrated in Figs. 4 and 5. For $^9\text{Be} + ^{40}\text{Ca}$ the RFRM fission barriers result in good agreement with the experimental fission cross section for L_{\max} smaller by only $2\hbar$ from the value predicted by the Bass model and Morgenstern *et al.* systematics. For the RLDM barriers, L_{\max} has to be increased by $11\hbar$ in order to get a similar result.

For $^6\text{Li} + ^{40}\text{Ca}$, the value of L_{\max} necessary to reproduce the experimental fission cross section is, respectively, larger by $5\hbar$ (RFRM barriers) or by $20\hbar$ (RLDM barriers) from the value suggested by the complete fusion cross section (67 ± 20 mb) measured for a similar reaction $^{26}\text{Li} + ^{46}\text{Ti}$ at the incident energy 156 MeV.

Calculations performed for three reactions $^6\text{Li}/^9\text{Be}/^{12}\text{C} + ^{49}\text{Ca}$ suggest a superiority of the RFRM barriers over the RLDM values. For the $^{32}\text{S} + ^{12}\text{C}$ system, both the RFRM and RLDM seem equally poor. The reason for this result being in contradiction with the other reactions investigated in this work may be due to an unknown systematic error in determination of σ_f , or from inadequacy of the Morgenstern *et al.* systematics or the Bass model to describe the inverse kinematic reaction of the $^{32}\text{S} + ^{12}\text{C}$ type.

We have tested two additional changes in parameters for these calculations. The first is to use a_f/a_v deduced from RLDM deformation parameters and the model of Bishop *et al.*²⁴ The result of this change is to increase fission yields by 30–40% over results with the parameters $\sigma_v = A/8$, $a_f = 1.02a_v$. The second point investigated was the effect of precompound nucleon emission preceding fission/evaporation competition. This tended to reduce the fission cross section by $\sim 30\%$ at the higher bombarding energy. In terms of changing the deduced L_{\max} parameters this brings σ_f calculated with RFRM barriers into close agreement with the Morgenstern *et al.* values, and moves results with the RLDM further away, insofar as this type of preequilibrium emission decay may not already be included in the Morgenstern systematics.

V. CONCLUSIONS

We have analyzed data for fission of light ($A < 52$) elements formed in heavy-ion bombardments via a Hauser-Feshbach/Bohr-Wheeler approach, using fission barriers based on the RLDM and RFRM. A reasonable range of level density parameters was used ($a_f/a_v = 0.98, 1.02$) and the maximum angular momentum for fusion L_{\max} was made a parameter. Using the RFRM, values of L_{\max} within a few units of results experimentally deduced or based on the systematics of Bass and of Morgenstern *et al.* gave satisfactory agreement with experimental yields. On the other hand, the RLDM generally required increases in L_{\max} in excess of $10\hbar$ (or 30–50% in L_{\max}) which is outside a reasonable change. These analyses therefore support the conclusion (consistent with that from heavier systems), that RFRM barriers are much nearer to experimentally deduced values than are those generated by the RLDM.

One of the authors (K.G.) wishes to acknowledge the hospitality of his colleagues at the Lawrence Livermore National Laboratory in Livermore, California.

- ¹K. Grotowski, Z. Majka, R. Planeta, M. Szczodrak, Y. Chan, G. Guarino, L. G. Moreto, D. J. Morrissey, L. G. Sobotka, R. G. Stokstad, I. Tserruya, S. Wald, and G. J. Wozniak, *Phys. Rev. C* **30**, 1214 (1984).
- ²R. Planeta, P. Belery, J. Brzychczyk, P. Cohilis, Y. El. Masri, G. Gregoire, K. Grotowski, Z. Majka, S. Mickek, M. Szczodrak, A. Wieloch, and J. Albinski, *Phys. Rev. C* **34**, 512 (1986).
- ³S. Cohen, F. Plasil, and W. J. Swiatecki, *Ann. Phys. (N.Y.)* **82**, 557 (1974).
- ⁴M. Beckerman and M. Blann, *Phys. Rev. C* **17**, 1615 (1978).
- ⁵M. Blann and T. A. Komoto, *Phys. Rev. C* **26**, 472 (1982).
- ⁶B. Sikora, W. Scobel, M. Beckerman, J. Bisplinghoff, and M. Blann, *Phys. Rev. C* **25**, 1446 (1982).
- ⁷G. Guillaume, J. P. Coffin, F. Rami, P. Engelstein, B. Heusch, P. Wagner, P. Fintz, J. Barrette, and H. E. Wegner, *Phys. Rev. C* **26**, 2458 (1982).
- ⁸D. J. Hinde, J. R. Leigh, J. O. Newton, W. Galster, and S. H. Sie, *Nucl. Phys. A* **385**, 109 (1982).
- ⁹H. J. Krappe, J. R. Nix, and A. J. Sierk, *Phys. Rev. C* **20**, 992 (1979).
- ¹⁰M. G. Mustafa, P. A. Baisden, and H. Chandra, *Phys. Rev. C* **25**, 2524 (1982).
- ¹¹A. J. Sierk, *Phys. Rev. C* **33**, 2039 (1986).
- ¹²J. van der Plicht, H. C. Britt, M. M. Gowler, Z. Fraenkel, A. Gavron, J. B. Wilhelmy, F. Plasil, T. C. Awes, and G. R. Young, *Phys. Rev. C* **28**, 2022 (1983).
- ¹³R. J. Charity, J. R. Leigh, J. J. M. Bokhorst, A. Chatterjee, G. S. Foote, D. J. Hinde, J. O. Newton, S. Ogaza, and D. Ward, *Nucl. Phys. A* **457**, 441 (1986).
- ¹⁴F. Plasil, T. C. Awes, B. Cheynis, D. Drain, R. L. Ferguson, F. E. Obenshain, A. J. Sierk, S. G. Steadman, and G. R. Young, *Phys. Rev. C* **29**, 1145 (1984).
- ¹⁵A. Gavron, J. Boissevain, H. C. Britt, K. Eskola, P. Eskola, M. M. Fowler, T. C. Awes, R. L. Ferguson, F. E. Obenshain, F. Plasil, G. R. Young, and S. Wald, *Phys. Rev. C* **30**, 1550 (1984).
- ¹⁶K. T. Lesko, W. Henning, K. E. Rehm, G. Rosner, J. P. Schiffer, G. S. F. Stephans, B. Zeidman, and W. S. Freeman, *Phys. Rev. Lett.* **55**, 803 (1985).
- ¹⁷M. A. McMahan, L. G. Moretto, M. L. Padgett, G. J. Wozniak, L. G. Sobotka, and M. G. Mustafa, *Phys. Rev. Lett.* **54**, 1995 (1985).
- ¹⁸R. J. Charity, M. A. McMahan, G. J. Wozniak, R. J. McDonald, L. G. Moretto, D. G. Sarantites, L. G. Sobotka, G. Guarino, A. Pantaleo, L. Fiore, A. Gobbi, and D. Hildenbrand, *Phys. Lett. B* (in press).
- ¹⁹U. L. Businaro and S. Gallone, *Nuovo Cimento* **1**, 629 (1955); **1**, 1277 (1955).
- ²⁰J. Błocki, K. Grotowski, R. Planeta, and W. J. Swiatecki, *Nucl. Phys.* **B445**, 367 (1985).
- ²¹M. Beckerman and M. Blann, University of Rochester Report No. UR-NSRL-135, 1977 (unpublished).
- ²²M. Blann and T. T. Komoto, Lawrence Livermore National Laboratory Report No. UCID-19390, 1982 (unpublished).
- ²³For references, see R. G. Stokstad, in *Heavy-Ion Science*, edited by D. A. Bromley (Plenum, New York, 1982).
- ²⁴C. J. Bishop, I. Halpern, R. W. Shaw, Jr., and R. Vandebosch, *Nucl. Phys. A* **193**, 161 (1972).
- ²⁵J. Brzychczyk, L. Freindl, K. Grotowski, Z. Majka, S. Micek, R. Planeta, M. Albinska, J. Buschmann, K. Klewe-Nebenius, H. J. Gils, H. Rebel, and S. Zagronski, *Nucl. Phys. A* **417**, 179 (1984).
- ²⁶R. Planeta *et al.*, *Nucl. Phys. A* **448**, 110 (1986).
- ²⁷R. Bass, *Nucl. Phys. A* **231**, 45 (1974), *Phys. Rev. Lett.* **39**, 265 (1977).
- ²⁸S. E. Vigdor, D. G. Kovar, P. Sperr, J. Mahoney, A. Menchanca-Rocha, C. Olmer, and M. S. Zisman, *Phys. Rev. C* **20**, 2147 (1979).
- ²⁹H. Morgenstern, W. Bohne, W. Galster, V. Grabisch, and A. Kyanowski, *Phys. Rev. Lett.* **52**, 1104 (1984).
- ³⁰K. Siwek-Wilczynska, E. H. du Marchie van Voorthuysen, J. van Popta, R. H. Siemssen, and J. Wilczynski, *Phys. Rev. Lett.* **42**, 1599 (1979).
- ³¹J. Wilczynski, K. Siwek-Wilczynska, J. Van Driel, S. Gonygrijp, D. C. J. M. Hageman, R. V. J. Janssen, J. Lukasiak, R. H. Siemssen, and S. Y. Van der Werf, *Nucl. Phys. A* **373**, 109 (1982).
- ³²K. A. Eberhard, C. Appel, R. Bangert, L. Cleemann, J. Eberth, and V. Zobel, in *Proceedings of the Second Louvain-Cracow Seminar on the Alpha-Nucleus Interaction*, Louvain-La-Neuve, 1978, edited by G. Gregoire, and K. Grotowski (unpublished).